Measurement of the High Q^2 Neutral Current DIS Cross Section with ZEUS at HERA

Matthias Moritz
(DESY)

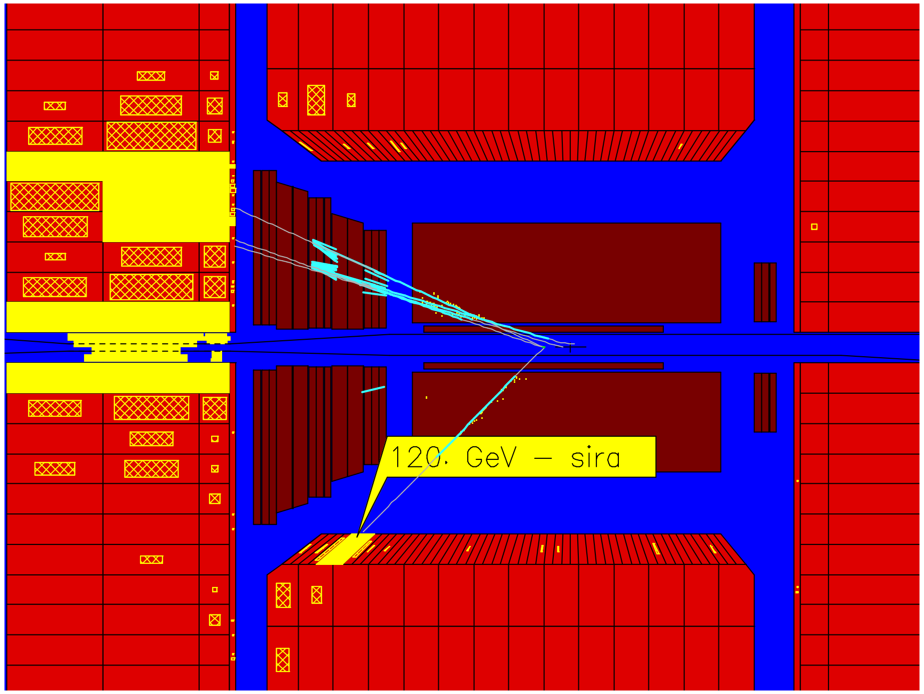

- Kinematics and Data Sets
- DIS Cross Section and Structure Functions
- High Q^2 NC Measurements with ZEUS
- Results: Cross Sections and xF_3
- Summary and Outlook

DIS ep scattering: Kinematics

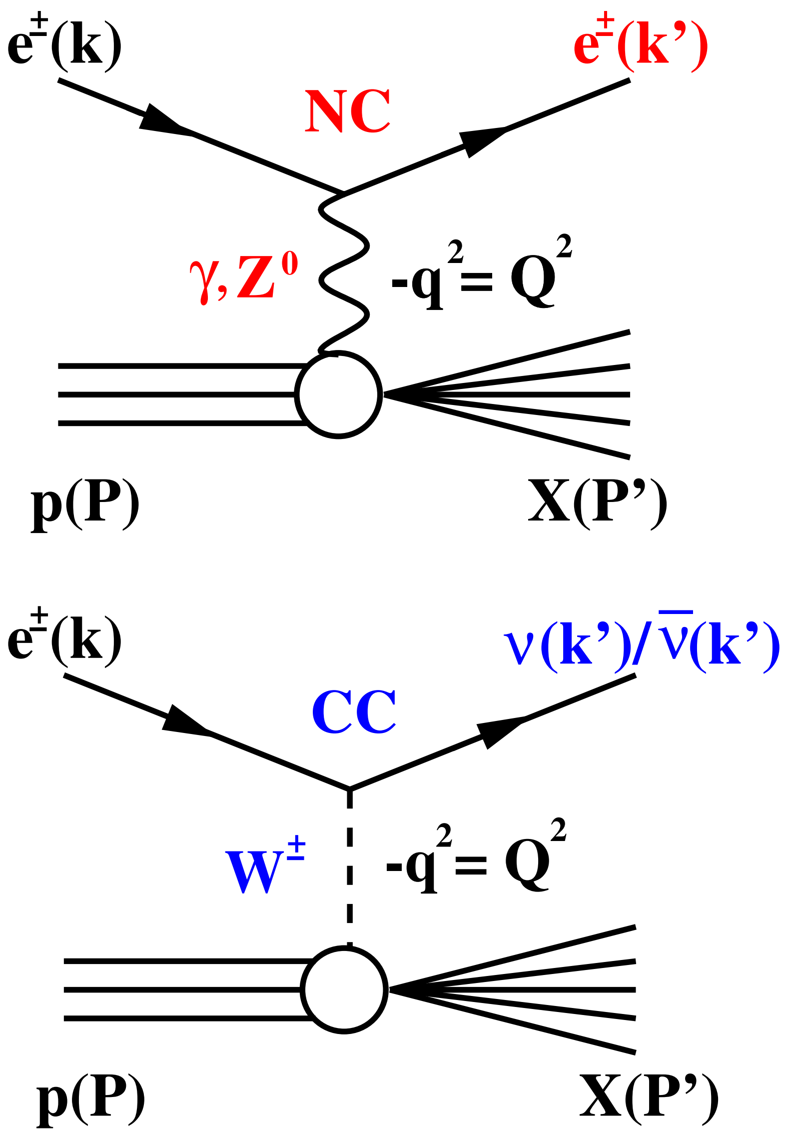

$$Q^2 = -q^2 = -(k - k')^2$$

negative four-momentum transfer, carried by boson

$$x = \frac{Q^2}{2P \cdot q}$$

QPM: fraction of proton momentum carried by struck quark

$$y = \frac{P \cdot q}{P \cdot k}$$

in eq cms: related to lepton scattering angle

$$s = (k + P)^2 = \frac{Q^2}{xy}$$

squared cms energy $\longrightarrow$ only two independent variables

DIS regime: $Q^2 \gg 1\,\mathrm{GeV}^2$

$\longrightarrow$ will look at $Q^2 > 185\,\mathrm{GeV}^2$

Photoproduction regime: $Q^2 \approx 0\,\mathrm{GeV}^2$

Kinematic Plane and Data Samples

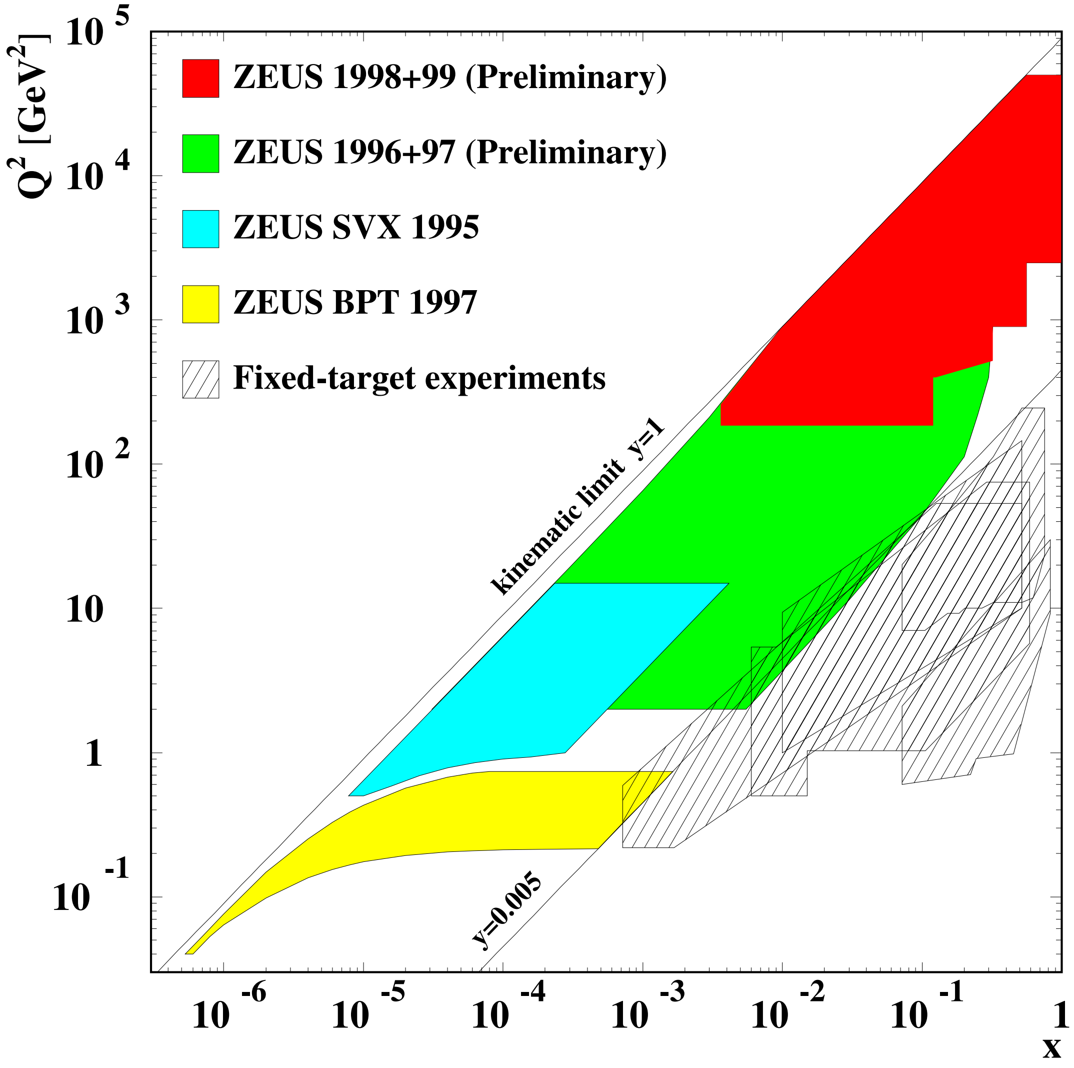

Run periods:

1994-1997	1998-1999	1999-2000
e^+p	e^-p	e^+p
$E_e = 27.5$ GeV	$E_e = 27.5$ GeV	$E_e = 27.5$ GeV
$E_p = 820$ GeV	$E_p = 920$ GeV	$E_p = 920$ GeV
$\sqrt{s} \approx 300$ GeV	$\sqrt{s} \approx 318$ GeV	$\sqrt{s} \approx 318$ GeV
$\mathcal{L} = 48\,\mathrm{pb}^{-1}$	$\mathcal{L} = 16\,\mathrm{pb}^{-1}$	$\mathcal{L} = 63\,\mathrm{pb}^{-1}$

- Preliminary Results of $(e^-p)^{920}$ and $(e^+p)^{920}$
- Extraction of the structure function $xF_3(x, Q^2)$ from $(e^-p)^{920}$ and $(e^+p)^{820}$

Cross Section and Structure Functions

Cross Section for $e^{\pm}p \rightarrow e^{\pm}X$:

$$\frac{d^2\sigma_{NC}^{e^{\pm}p}}{dx\,dQ^2} = \frac{2\pi\alpha^2}{Q^4 x}\left[Y_{(+)}F_2^{NC} \mp Y_{(-)}xF_3^{NC} - y^2 F_L^{NC}\right]$$

with $Y_{(\pm)} = 1 \pm (1-y)^2$

reduced Xsect:

$$\tilde{\sigma}_{NC}^{e^{\pm}p} = F_2^{NC} \mp \frac{Y_{(-)}}{Y_{(+)}} xF_3^{NC} - \frac{y^2}{Y_{(+)}} F_L^{NC}$$

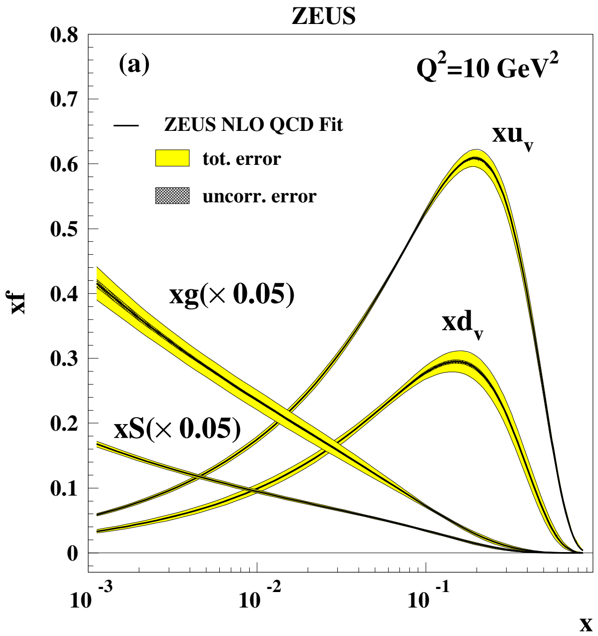

$F_2(x,Q^2) = \sum_i x(q+\bar{q})A_i$

F_2 : sensitive to valence- and seaquark distribution, dominant contribution to cross section

$xF_3(x,Q^2) = \sum_i x(q-\bar{q})B_i$

xF_3 :parity violating part, sensitive only to valence quark distribution, contributes at high Q^2

F_L :describes absorption of longitudinally polarised photon $\rightarrow = 0$ in QPM; in NLO: small at high Q^2

The couplings in detail:

$$A_q = e_q^2 - 2e_q v_q v_l \chi_Z + (v_q^2 + a_q^2)(v_l^2 + a_l^2)\chi_Z^2 \qquad \text{and} \qquad B_q = -2e_q a_q a_l \chi_Z + 4v_q a_q v_l a_l \chi_Z^2$$

with

$$a_f = t_3^f \quad \text{and} \quad v_f = t_3^f - 2e_f \sin^2\theta_W$$

$$\chi_Z = \frac{1}{4\sin^2\theta_W \cos^2\theta_W} \cdot \left(\frac{Q^2}{M_Z^2 + Q^2}\right) = \kappa_W \cdot \left(\frac{Q^2}{M_Z^2 + Q^2}\right)$$

The structure functions as a function of the individual process:

$$F_2 = F_2^{em} - v_l \left[\frac{\kappa_W Q^2}{Q^2 + M_Z^2}\right] G_2 + (v_l^2 + a_l^2)\left[\frac{\kappa_W Q^2}{Q^2 + M_Z^2}\right]^2 H_2$$

$$xF_3 = -a_l \left[\frac{\kappa_W Q^2}{Q^2 + M_Z^2}\right] xG_3 + 2a_l v_l \left[\frac{\kappa_W Q^2}{Q^2 + M_Z^2}\right]^2 xH_3$$

where the functions $G_{2,3}$ arise from $\gamma - Z$ interference and $H_{2,3}$ from pure Z exchange

$\rightarrow$ High Q^2 measurements test electro-weak and QCD sector of Standard Model

NC event in the ZEUS detector

Main components of the ZEUS detector:

CTD (wire chamber): tracking information

FCAL, BCAL and RCAL: compensating sampling calorimeter: energy information

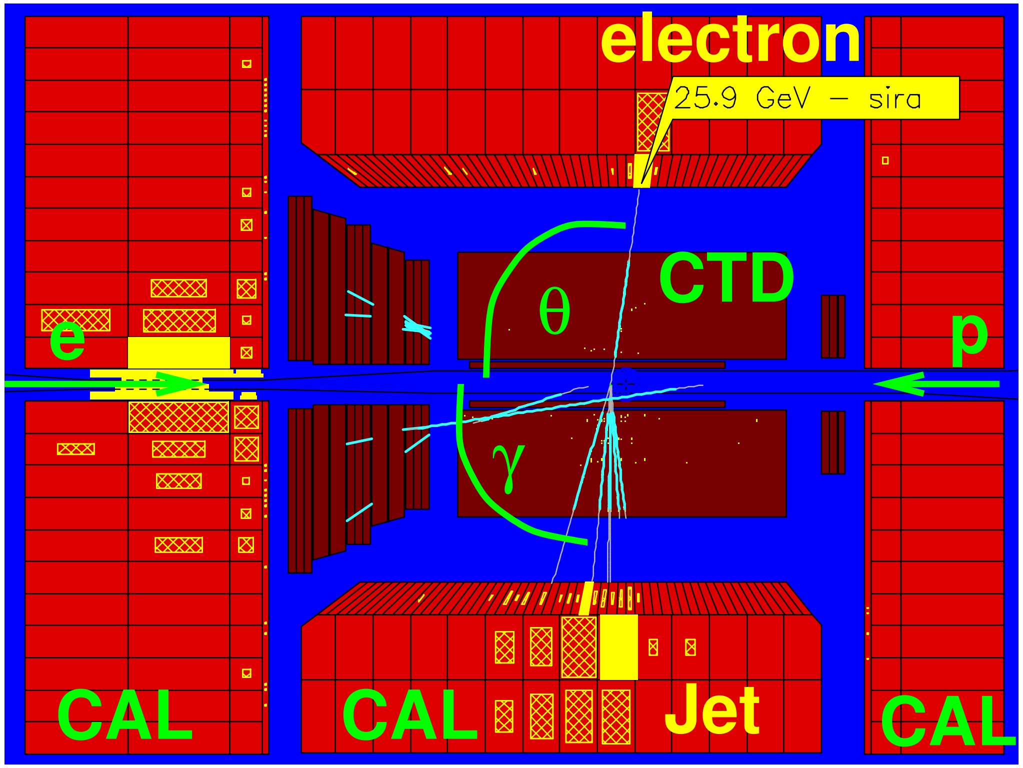

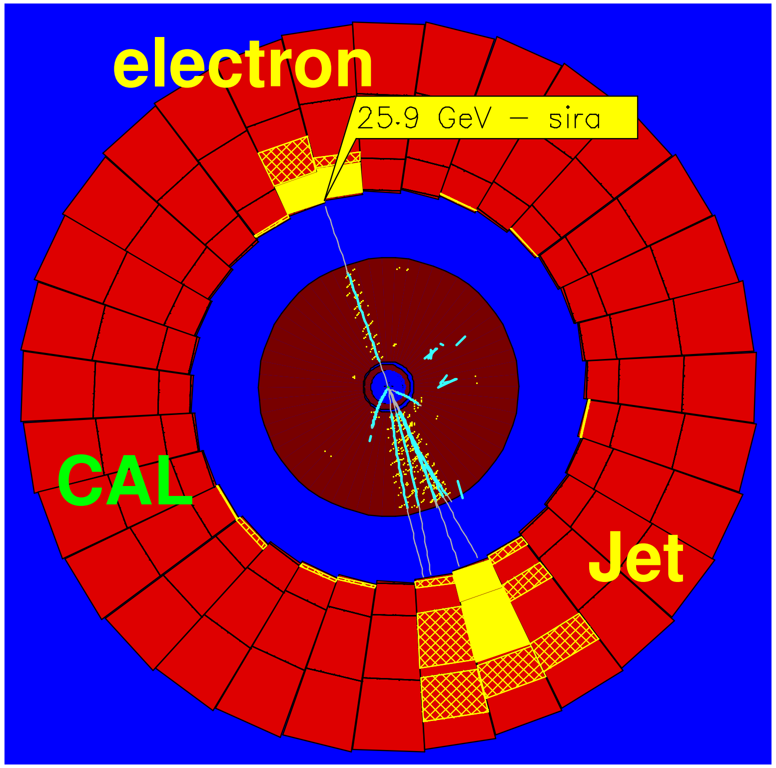

- scattered electron and hadronic jet balance in transverse momentum

Event Selection and Reconstruction Method

- Electron identification
  - Electron energy: $E_e > 10$ GeV
  - Isolation: $E_{CONE} < 5$ GeV
  - Matched electron track with $P_{trk} > 5$ GeV ($\theta_e > 17°$)
  - low θ: $p_{T,e} = E_e \sin(\theta) > 30$ GeV
- Z-vertex close to IP: -50 cm$<$ Z $<$ 50 cm
- Background suppression:

  $$(E - p_Z)_{ini} = 920\,\mathrm{GeV} + 27.5\,\mathrm{GeV} - (920\,\mathrm{GeV} - 27.5\,\mathrm{GeV}) = 55\,\mathrm{GeV} \rightarrow \text{conserved!}$$

  - 38 (44) GeV $< E - p_Z <$ 65 GeV
  - $y_E <$ 0.95
  - Balance of transverse momentum $p_T/\sqrt{E_T} < 4\,\sqrt{\mathrm{GeV}}$
- Kinematic Reconstruction: Double Angle Method
- Kinematic Range: 185 GeV^2 $< Q^2 <$50000 GeV^2

Control Plots (e^+p 99/00)

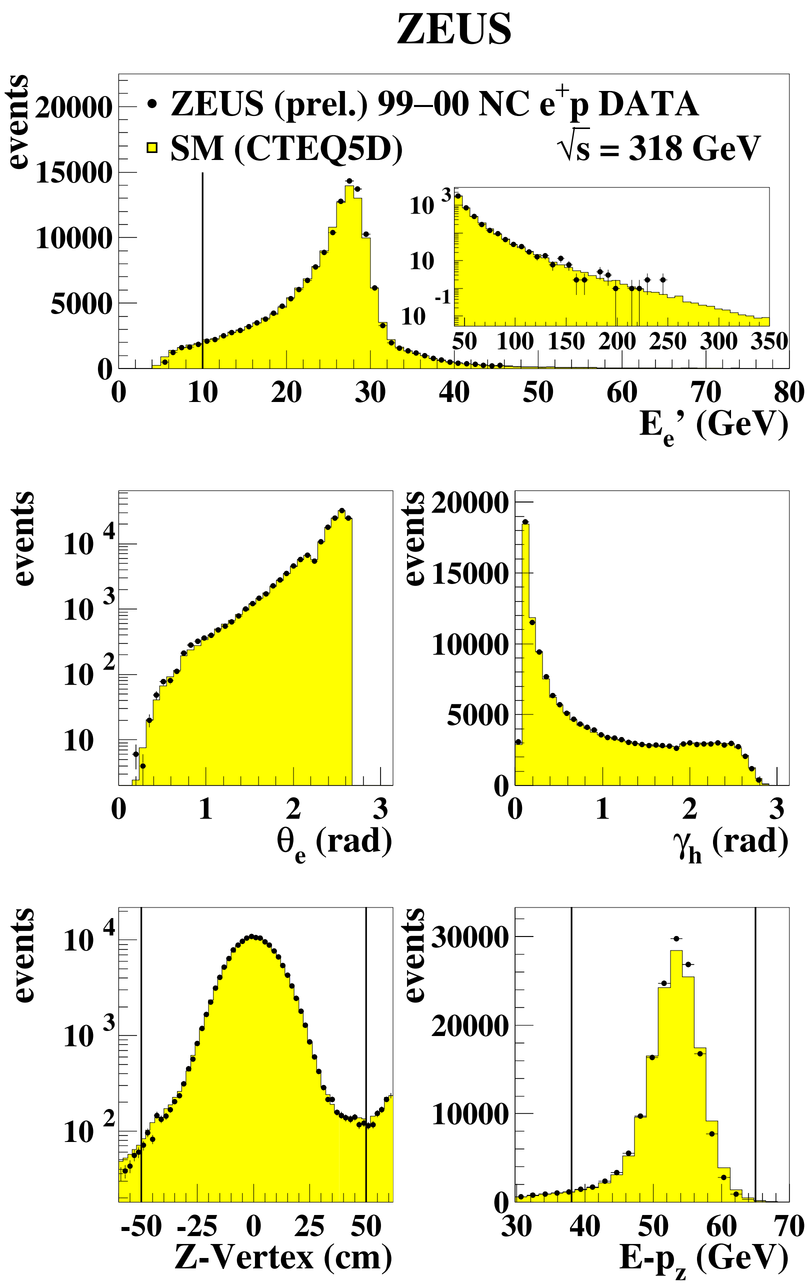

Control Plots of

- Scattered electron energy
- scattering angles
- longitudinal interaction point
- $E - p_Z$ distribution

- MC PDF input: CTEQ5D
- Data well described by MC
- also good agreement for 98/99 e^-p

Results: Single Differential Cross Section $d\sigma^{e^{\pm}p}/dQ^2$

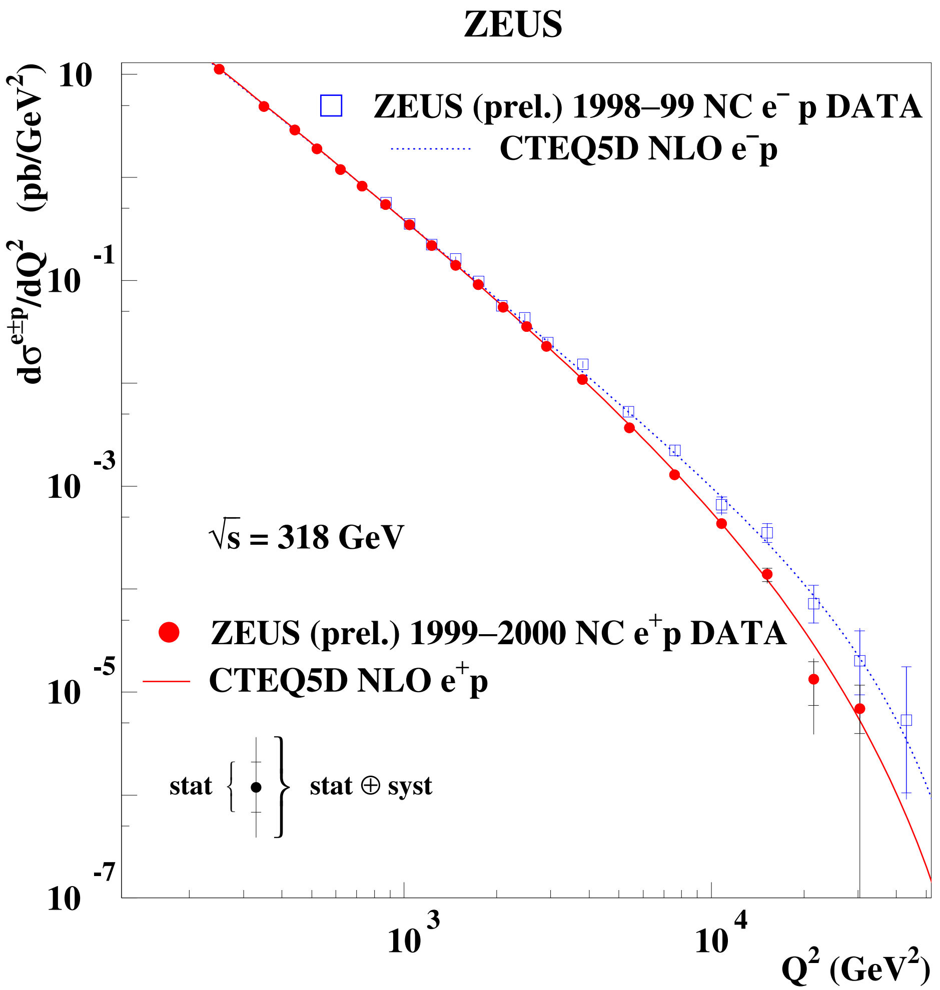

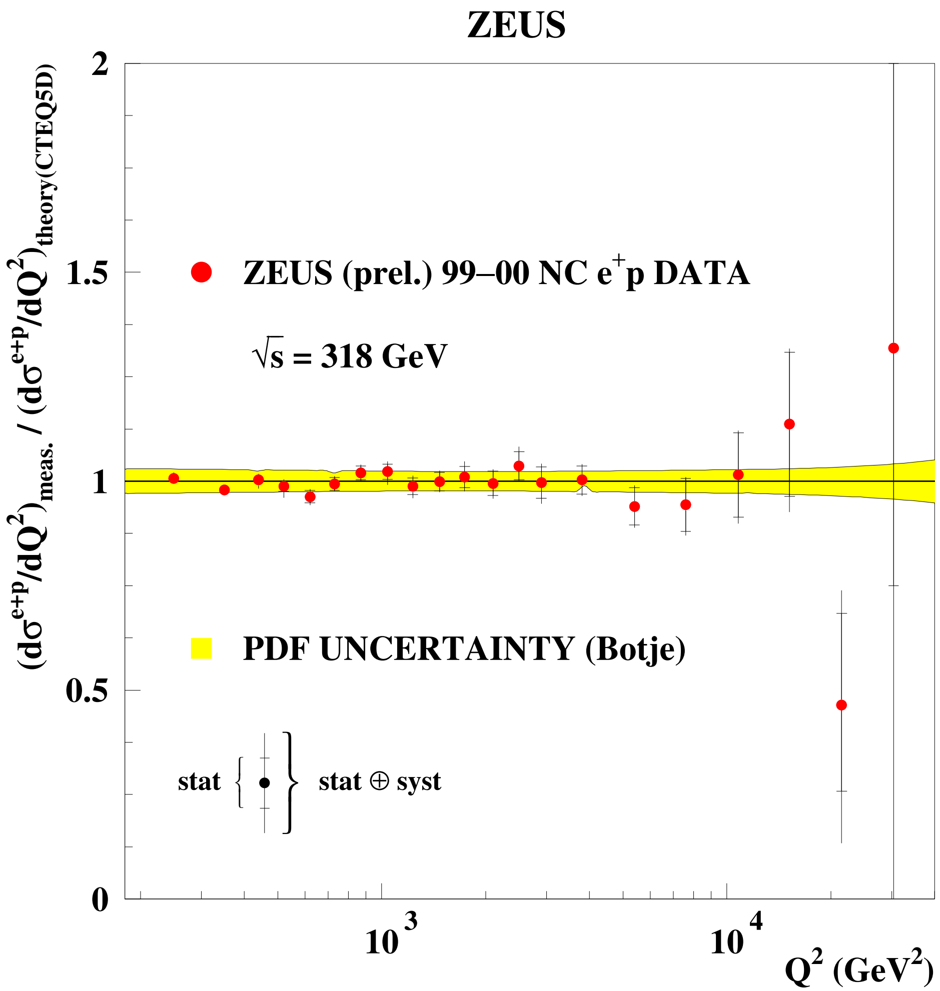

- $Q^2 \leq 1000\,\mathrm{GeV}^2$ γ exchange is dominating
- larger Q^2: γ–Z^0 interference becomes visible
- resolvable distances of $\mathcal{O}$ (1/1000) of proton radius
- good description by Standard Model

Single Differential Cross Section $d\sigma^{e^+p}/dx$ and $d\sigma^{e^+p}/dy$

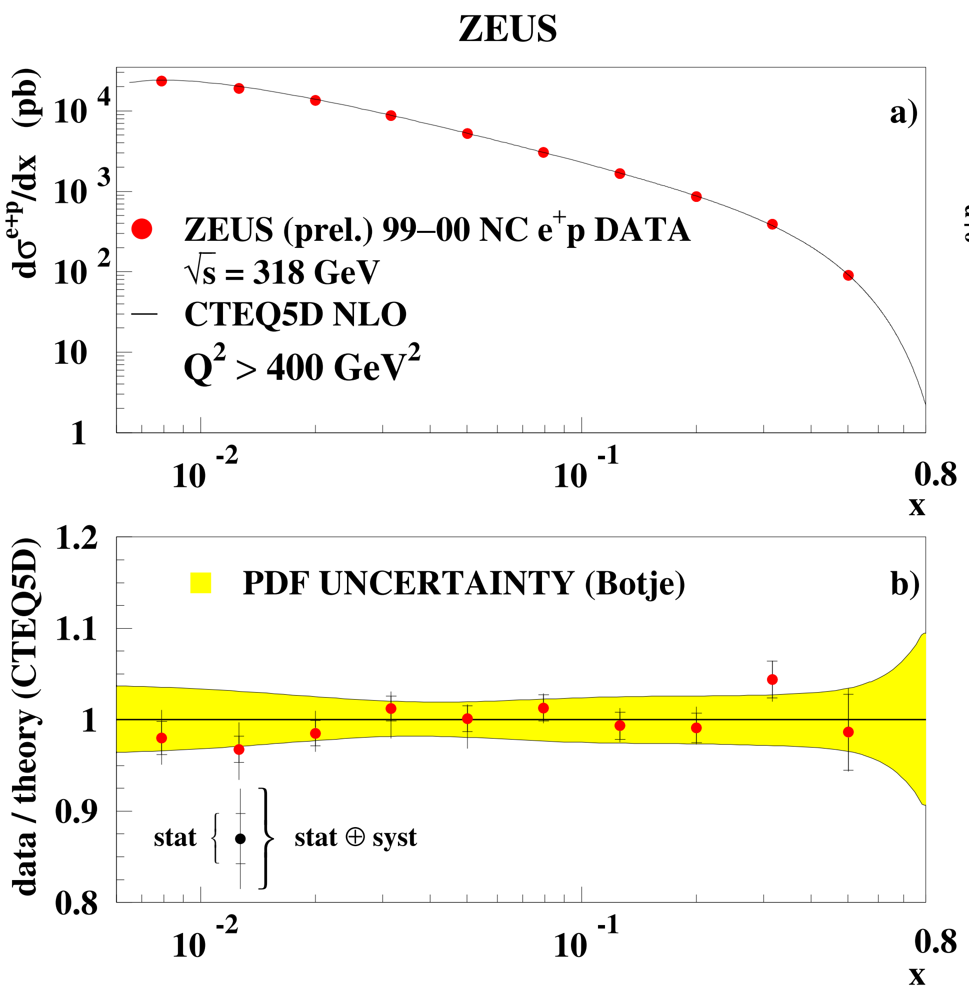

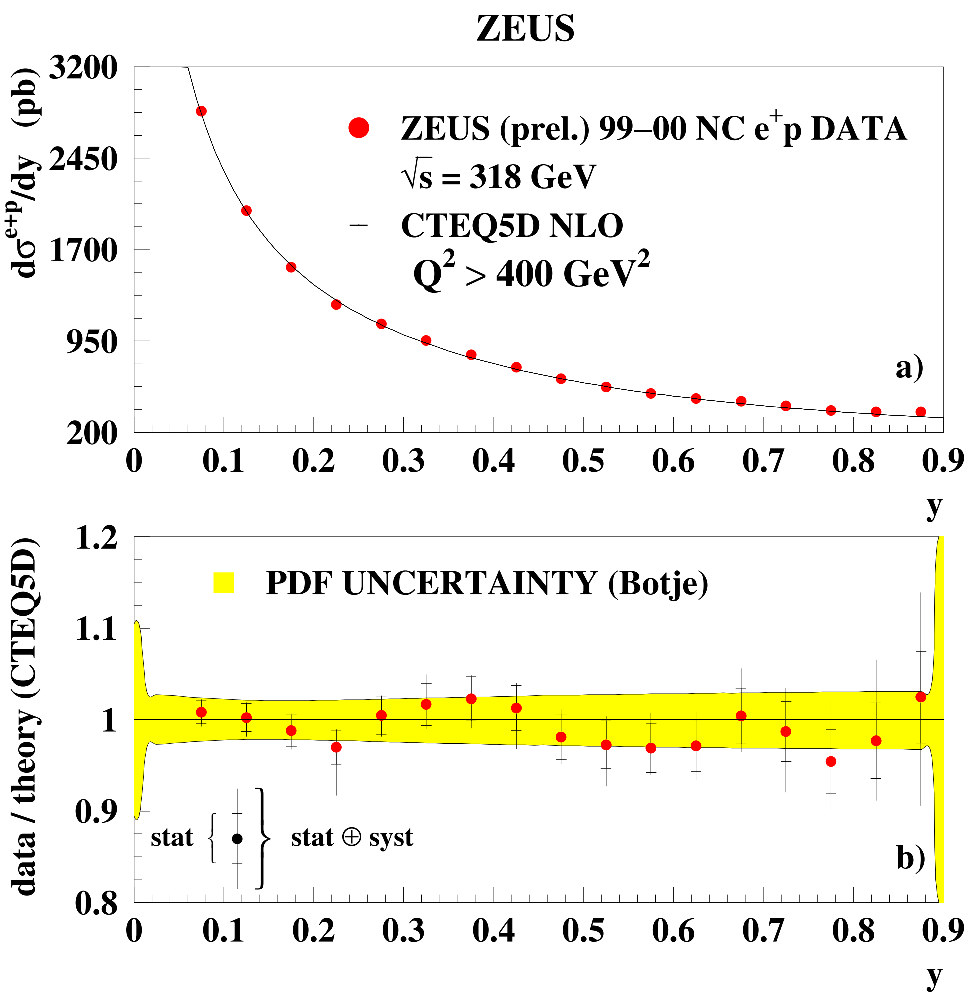

- Data well described by Standard Model
- Data well understood in all three kinematic variables

Single Differential Cross Section $d\sigma^{e^+p}/dx$ at high Q^2

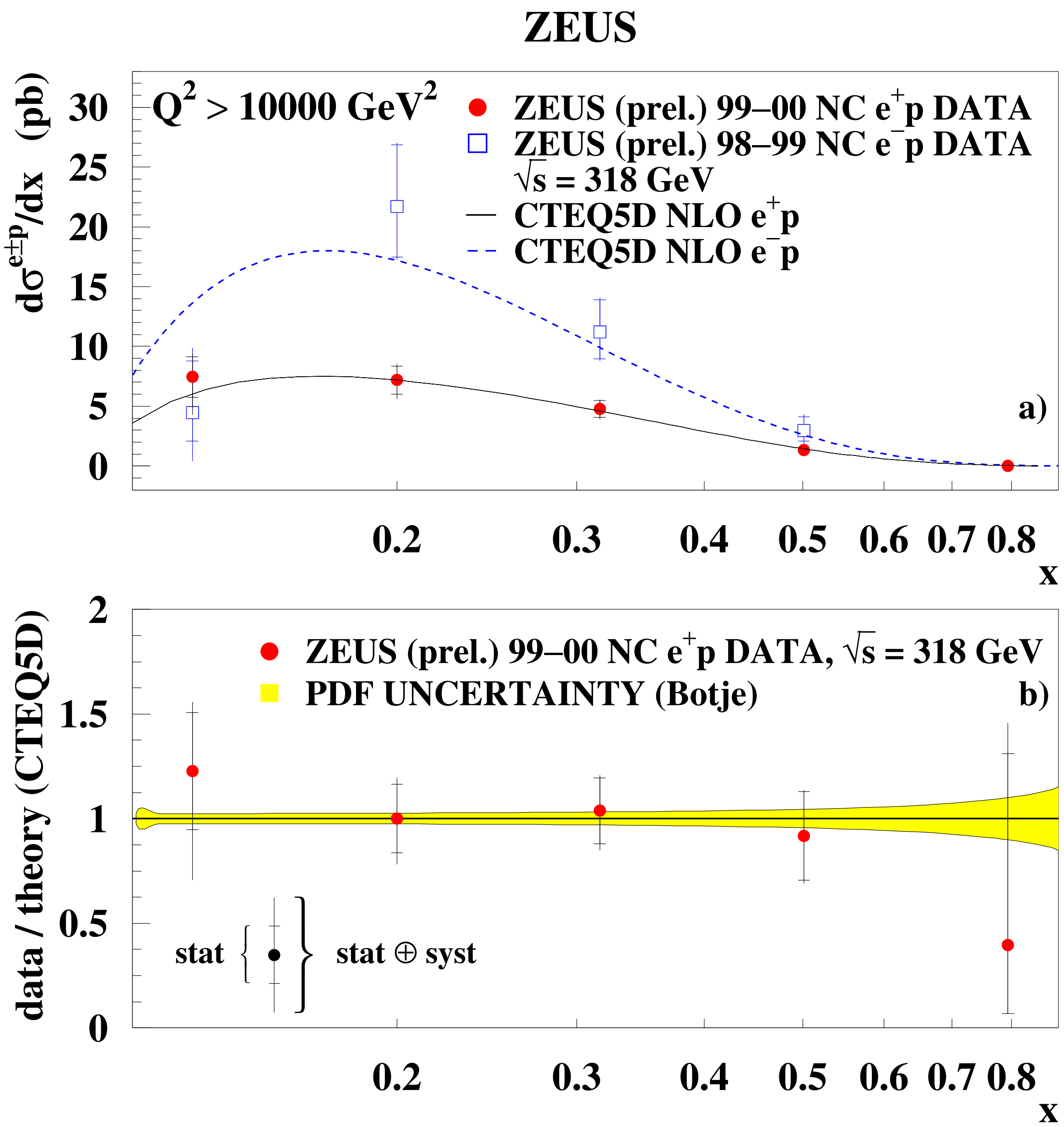

γ–Z^0 interference at high Q^2:

- constructive for e^-p data
- destructive for e^+p data

Results: Reduced Double Differential Cross Section $\tilde{\sigma}_{NC}^{e^{\pm}p} \approx F_2^{NC} \mp \frac{Y_{(-)}}{Y_{(+)}} xF_3^{NC}$

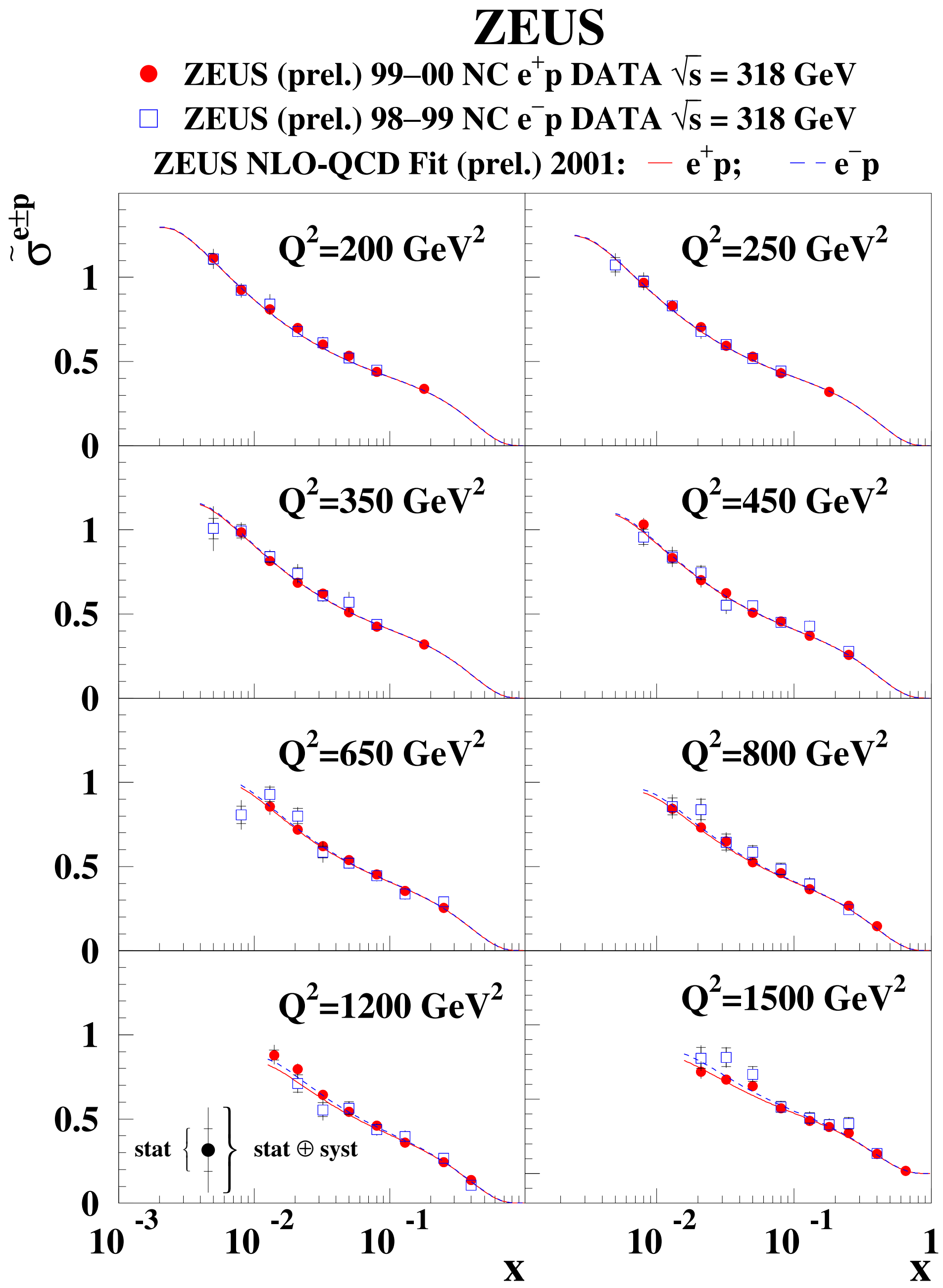

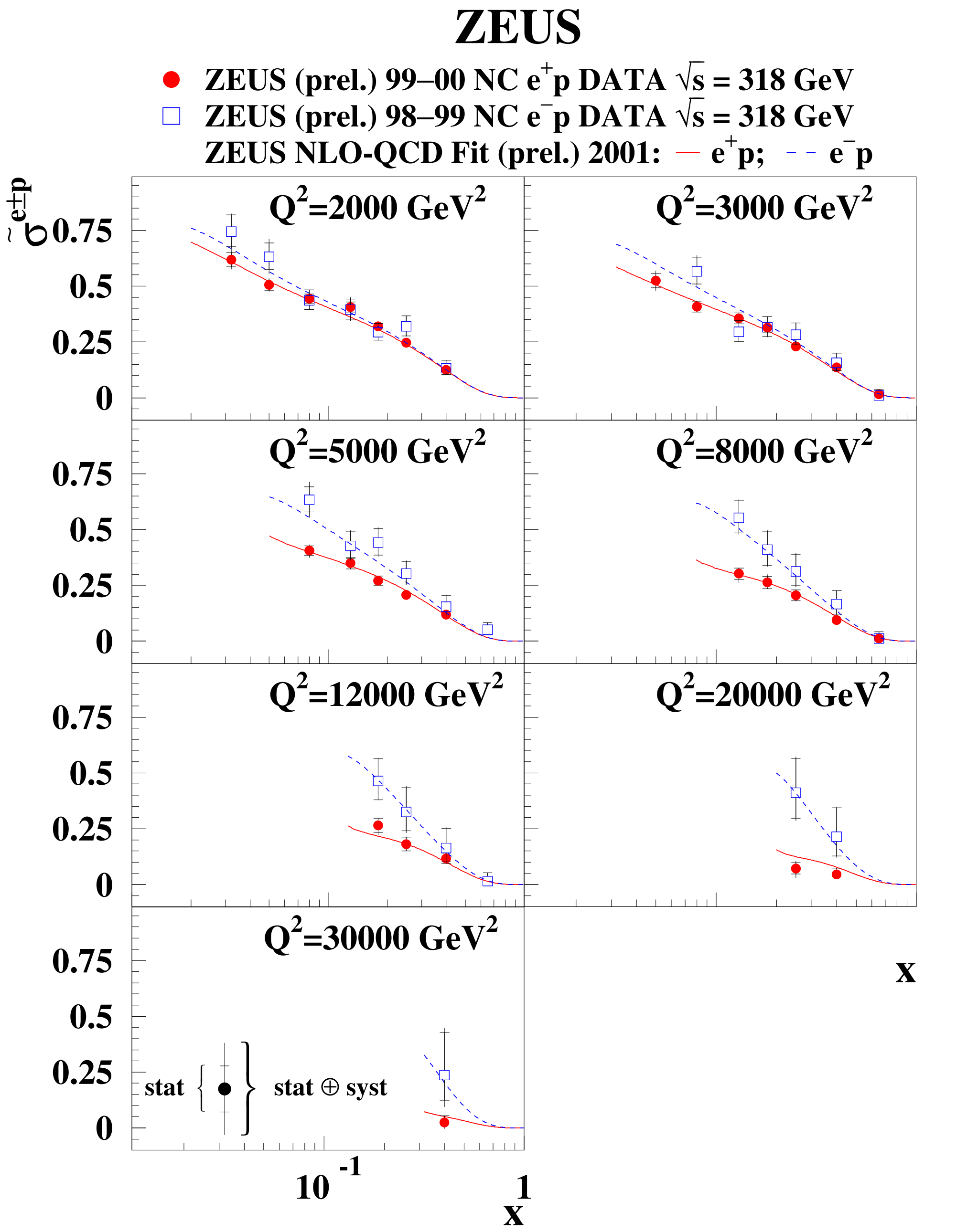

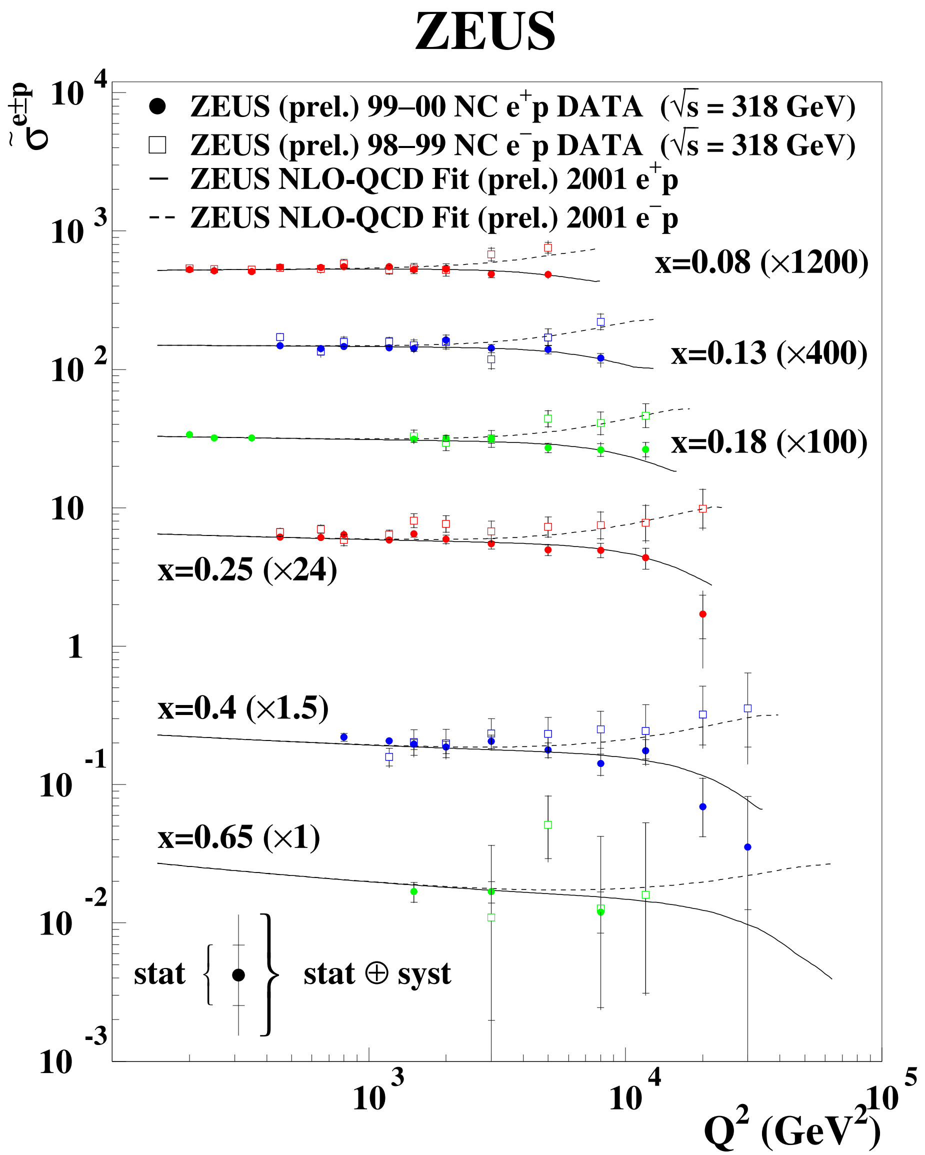

- e^+p and e^-p cross sections similar at low Q^2
  $\rightarrow$ photon exchange
- e^+p and e^-p cross sections differ from $Q^2 \approx 3000$ GeV^2
  $\rightarrow$ $\gamma - Z$ interference
- high Q^2 dependence well described by Standard Model
- combination of e^+p and e^-p data
  $\rightarrow$ extraction of structure function xF_3

Results: Extraction of the Structure Function xF_3 ($\sim \sum_i x(q-\bar{q})$)

Extraction of xF_3 with $(e^- p)^{920}$ and $(e^+ p)^{820}$

$$\frac{d^2\sigma_{NC}^{e^\pm p}}{dx dQ^2} = \frac{2\pi\alpha^2}{Q^4 x}[Y_{(+)}F_2 \mp Y_{(-)} xF_3 - y^2 F_L]$$

Take into account different center-of-mass energy

$$xF_3(x,Q^2) = \left(\frac{xQ^2}{2\pi\alpha^2}\right)\left(\frac{Y_{(-)}^{920}}{Y_{(+)}^{920}} + \frac{Y_{(-)}^{820}}{Y_{(+)}^{820}}\right)^{-1}$$

$$\cdot\left(\frac{1}{Y_{(+)}^{920}}\frac{d^2\sigma^-}{dx dQ^2} - \frac{1}{Y_{(+)}^{820}}\frac{d^2\sigma^+}{dx dQ^2}\right) - \Delta F_L$$

with

$$\Delta F_L = \frac{Y_{(+)}^{820}\cdot(y^{920})^2 - Y_{(+)}^{920}\cdot(y^{820})^2}{Y_{(-)}^{920}\cdot Y_{(+)}^{820} + Y_{(-)}^{820}\cdot Y_{(+)}^{920}}\cdot F_L(x,Q^2)$$

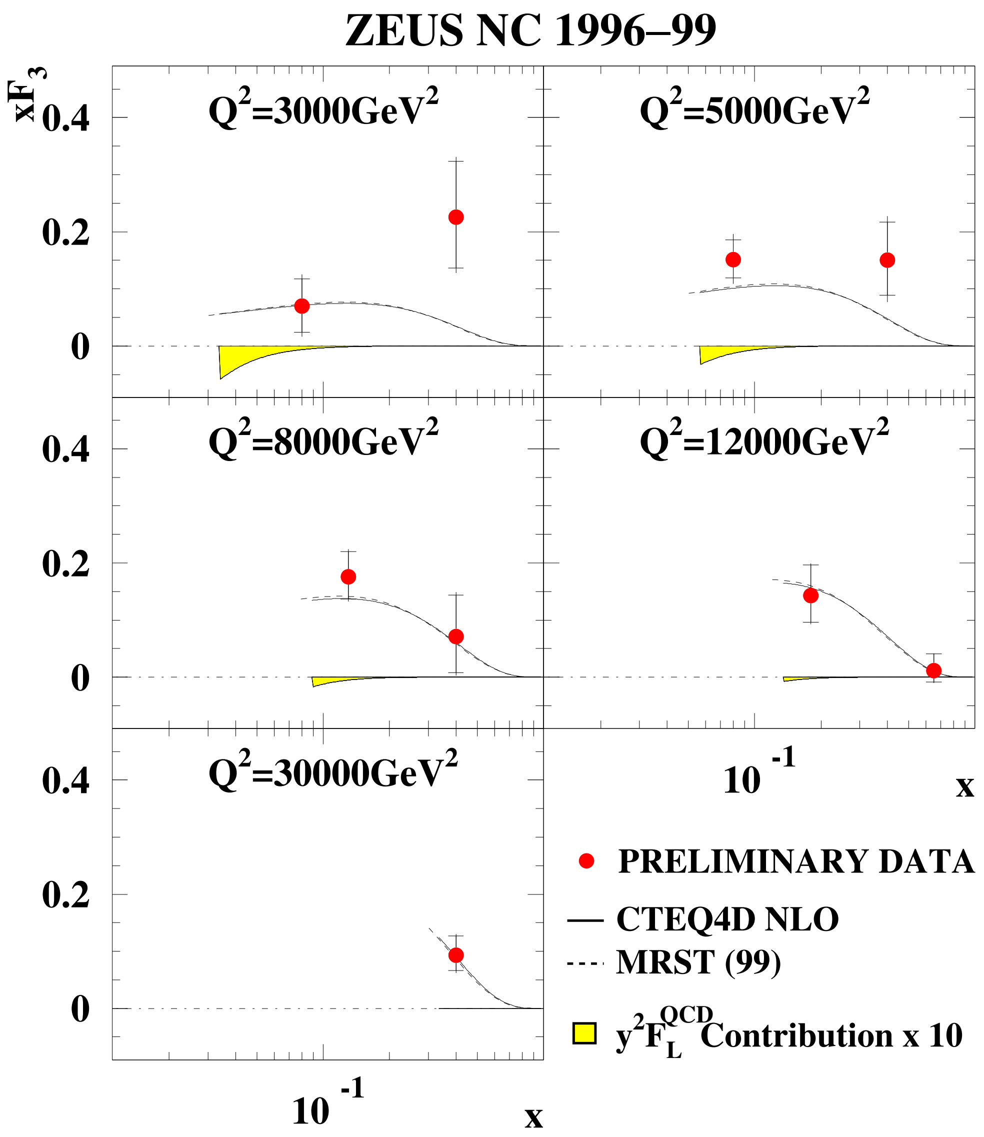

Towards Final Results: Work on Systematic Uncertainties

- Uncertainty of the electron energy scale:
  $3\% \rightarrow 1-2\%$(BCAL/RCAL)
- Uncertainty of the hadronic energy scale
  $2-3\% \rightarrow 1-2\%$
- Number of backgound photoproduction events
  normalisation study reduced uncertainty(reduction $> 50\%$)
- Uncertainty of the fragmentation model (CDM $\leftrightarrow$ MEPS)
  uncertainty determined by detailed energy flow study (reduction by $\sim 50\%$)

$\rightarrow$ ZEUS final results expected soon!

Summary and Outlook

Analysis of high Q^2 NC 98/99 e^-p and 99/00 e^+p data set shows:

- the most precise look into the proton structure at length scales of $\mathcal{O}(1/1000)$ proton radius to date
- good description of the data by the Standard Model up to highest values of Q^2
- the valence quark distribution via the Structure Function xF_3(in combination with 96/97 e^+p)

ZEUS final results expected soon

- last HERA measurement with unpolarised lepton beams $\longrightarrow$ reference for measurements after the HERA upgrade
- NC analyses at HERA Run 2: $\longrightarrow$ Structure function measurements with higher statistics $\longrightarrow$ more precise constrains on PDFs

  $\longrightarrow$ different lepton polarisation $\longrightarrow$ studies of electroweak effects